British Journal of Pharmacology

DOI:10.1111/j.1476-5381.2012.02015.x
www.brjpharmacol.org

RESEARCH PAPER

Role of action potential configuration and the contribution of Ca^{2+} and K^+ currents to isoprenaline-induced changes in canine ventricular cells

N Szentandrássy[1]*, V Farkas[2]*, L Bárándi[1], B Hegyi[1], F Ruzsnavszky[1], B Horváth[1], T Bányász[1], J Magyar[1], I Márton[2] and PP Nánási[1]

[1]*Department of Physiology, University of Debrecen, Debrecen, Hungary, and* [2]*Department of Dentistry, University of Debrecen, Debrecen, Hungary*

Correspondence
Péter P. Nánási, Department of Physiology, University of Debrecen, Nagyerdei krt 98, H-4012 Debrecen, Hungary. E-mail: nanasi.peter@med.unideb.hu; nanasi@phys.dote.hu

*The first two authors (NS and VF) have equally contributed.

Keywords
β-adrenergic activation; isoprenaline; action potential configuration; calcium current; potassium currents; ventricular repolarization; dog myocytes

Received
30 March 2012
Accepted
24 April 2012

BACKGROUND AND PURPOSE

Although isoprenaline (ISO) is known to activate several ion currents in mammalian myocardium, little is known about the role of action potential morphology in the ISO-induced changes in ion currents. Therefore, the effects of ISO on action potential configuration, L-type Ca^{2+} current (I_{Ca}), slow delayed rectifier K^+ current (I_{Ks}) and fast delayed rectifier K^+ current (I_{Kr}) were studied and compared in a frequency-dependent manner using canine isolated ventricular myocytes from various transmural locations.

EXPERIMENTAL APPROACH

Action potentials were recorded with conventional sharp microelectrodes; ion currents were measured using conventional and action potential voltage clamp techniques.

KEY RESULTS

In myocytes displaying a spike-and-dome action potential configuration (epicardial and midmyocardial cells), ISO caused reversible shortening of action potentials accompanied by elevation of the plateau. ISO-induced action potential shortening was absent in endocardial cells and in myocytes pretreated with 4-aminopyridine. Application of the I_{Kr} blocker E-4031 failed to modify the ISO effect, while action potentials were lengthened by ISO in the presence of the I_{Ks} blocker HMR-1556. Both action potential shortening and elevation of the plateau were prevented by pretreatment with the I_{Ca} blocker nisoldipine. Action potential voltage clamp experiments revealed a prominent slowly inactivating I_{Ca} followed by a rise in I_{Ks}, both currents increased with increasing the cycle length.

CONCLUSIONS AND IMPLICATIONS

The effect of ISO in canine ventricular cells depends critically on action potential configuration, and the ISO-induced activation of I_{Ks} – but not I_{Kr} – may be responsible for the observed shortening of action potentials.

Abbreviations

APD_{90}: action potential duration measured at 90% repolarization; E 4031, 1-[2-(6-methyl-2pyridyl)ethyl]-4-(4-methylsulfonyl aminobenzoyl)piperidine; HMR 1556, (3R,4S)-(+)-*N*-[3-hydroxy-2,2-dimethyl-6-(4,4,4-trifluorobutoxy) chroman-4-yl]-*N*-methylethanesulfonamide; I_{Ca}, L-type Ca^{2+} current; I_{Kr}, rapid component of delayed rectifier K^+ current; I_{Ks}, slow component of delayed rectifier K^+ current; I_{Kto}, transient outward K^+ current; I_{Cl}, Cl^- current; ISO, isoprenaline

Introduction

β-Adrenoceptor-mediated activation of cardiac tissues is considered as one of the most important adaptive mechanisms in the mammalian heart. The positive tropic effects of adrenoceptor activation are associated with a marked increase in I_{Ca} (Dukes and Vaughan Williams, 1984; McDonald *et al.*, 1994). This extra inward current has to be compensated for by a concomitant increase in outward currents in cardiac tissues exposed to sympathetic stimulation or isoprenaline (ISO) in order to minimize the pro-arrhythmic effects of enhanced sympathetic activity (January and Riddle, 1990). Indeed, in addition to the increase of I_{Ca} (Van der Heyden *et al.*, 2005), ISO-induced activation of a slow delayed rectifier K^+ current (I_{Ks}) (Stengl *et al.*, 2003; Volders *et al.*, 2003; Rocchetti *et al.*, 2006), fast delayed rectifier K^+ current (I_{Kr}) (Heath and Terrar, 2000; Harmati *et al.*, 2011) and chloride current (I_{Cl}) (Harvey *et al.*, 1990) has been demonstrated in various mammalian cardiac preparations. In spite of the huge amounts of data obtained on the cardiac effects of β-adrenoceptor-mediated activation at an ion current level, little is known about the relationship between action potential morphology and the ISO-induced changes in canine ventricular cells. In addition, there are marked interspecies differences between the effects of ISO on action potential duration including both prolongation (Belardinelli and Isenberg, 1983; Taggart *et al.*, 1990; Rocchetti *et al.*, 2006; Ogura *et al.*, 2007) as well as shortening (Dukes and Vaughan Williams, 1984; Malfatto *et al.*, 1993; Ruiz Petrich *et al.*, 1996; Dorian *et al.*, 2002; Taggart *et al.*, 2003; Volders *et al.*, 2003) of action potentials. Thus, the question arises as to whether these differences in ISO effects are a consequence of different kinetic properties of the underlying current systems or are related to variations in action potential morphology. Furthermore, the relative contribution of I_{Kr} in compensating for the ISO-induced augmentation of I_{Ca} in dog heart has not been explored. Therefore, in the present study, β-adrenoceptor stimulation was affected by application of 10–100 nM of ISO, which is known to induce close to maximal effects in cardiac cells (Katsube *et al.*, 1996). The effects of ISO on action potential configuration, and on the profiles of the most important ISO-modulated ion currents, including I_{Ca}, I_{Ks} and I_{Kr}, were studied separately in canine isolated ventricular myocytes, under action potential voltage clamp conditions and in a frequency-dependent manner. The role of action potential configuration was studied using myocytes of epicardial and endocardial origin; furthermore, epicardial cells were converted to display endocardial-like action potentials by suppressing the transient outward K^+ current (I_{Kto}) pharmacologically. The question, whether all ISO-induced changes are mediated through one common signal transduction pathway, was also addressed. The significance of studying canine cells is supported by evidence showing that ventricular ion currents in the human heart strongly resemble those found in canine myocardium (Szabó *et al.*, 2005; Szentadrássy *et al.*, 2005; Jost *et al.*, 2009). Our results revealed that (i) the effect of ISO on the parameters of the action potential critically depend on the shape of the action potential; (ii) the ISO-induced activation of I_{Ks} – but not I_{Kr} – is the main mechanism responsible for the ISO-induced shortening of action potential in dogs; and (iii) all ISO-induced currents are stimulated through the same single mechanism.

Methods

Isolation of single canine ventricular myocytes

Adult beagle dogs of either sex were anaesthetized with i.m. injections of 10 mg·kg^{-1} ketamine hydrochloride (Calypsol, Richter Gedeon, Hungary) +1 mg·kg^{-1} xylazine hydrochloride (Sedaxylan, Eurovet Animal Health BV, the Netherlands) according to a protocol approved by the local ethical committee, which conformed to the principles outlined in the Declaration of Helsinki. The hearts were quickly removed and placed in Tyrode solution. Single myocytes were obtained by enzymatic dispersion using the segment perfusion technique (Magyar *et al.*, 2002; Szentandrássy *et al.*, 2011). Briefly, a wedge-shaped section of the ventricular wall supplied by the left anterior descending coronary artery was dissected, cannulated and perfused with oxygenized Tyrode solution containing (in mM) NaCl, 144; KCl, 5.6; $CaCl_2$, 2.5; $MgCl_2$, 1.2; HEPES, 5; and dextrose, 11; at pH = 7.4. Perfusion was maintained until the removal of blood from the coronary system and then switched to a nominally Ca^{2+}-free Joklik solution (Minimum Essential Medium Eagle, Joklik Modification, Sigma-Aldrich Co., St. Louis, MO, USA) for 5 min. This was followed by 30 min perfusion with Joklik solution supplemented with 1 mg·mL^{-1} collagenase (Type II, Worthington Chemical Co., Lakewood, NJ, USA) and 0.2% BSA (Fraction V., Sigma) containing 50 μM Ca^{2+}. Full transmural sections of the middle portion of the left ventricular wall were cut into small pieces and the cell suspension was washed with Joklik solution. These tissue chunks contained predominantly mid-myocardial myocytes. In some experiments (as indicated), cells were obtained specifically from the subepicardial or subendocardial layers of the heart by carefully slicing the left ventricular free wall. Finally, the Ca^{2+} concentration was gradually restored to 2.5 mM. The cells were stored in Minimum Essential Eagle's Medium until use.

Experiments were performed on 157 canine ventricular cells derived from a total of 39 animals. All the studies involving animals are reported in accordance with the ARRIVE guidelines (Kilkenny *et al.*, 2010; McGrath *et al.*, 2010).

Recording of action potentials

All electrophysiological measurements were performed at 37°C. The rod-shaped viable cells showing clear striation were sedimented in a Plexiglas chamber allowing continuous superfusion with oxygenated Tyrode solution. Transmembrane potentials were recorded using 3 M KCl-filled sharp glass microelectrodes having tip resistance between 20 and 40 MΩ. These electrodes were connected to the input of an Axoclamp-2B amplifier (Axon Instruments Inc., Foster City, CA, USA). The cells were paced through the recording electrode at a steady cycle length of 1 s using 1 ms wide rectangular current pulses with an amplitude twice that of the diastolic threshold. Since the cytosol was not dialysed, time-dependent changes in action potential duration were negligible for at least 60 min under these experimental conditions

(Horváth *et al.*, 2006). ISO was applied in a cumulative manner (at each exposure for 2 min) followed by a 10-min period of washout. Action potentials were digitized at 200 kHz using Digidata 1200 A/D card (Axon Instruments) and stored for later analysis.

Conventional voltage clamp

The cells were superfused with oxygenated Tyrode solution at 37°C. This superfusate was supplemented with 1 μM E 4031 plus 5 μM nisoldipine when measuring I_{Ks}, or 10 μM HMR 1556 plus 5 μM nisoldipine when measuring I_{Kr}, while 1 μM E 4031, 10 μM HMR 1556 and 3 mM 4-aminopyridine were present extracellularly in case of I_{Ca} recording. Suction pipettes, made of borosilicate glass, had tip resistances of 2 MΩ after being filled with pipette solution containing (in mM) K-aspartate, 100; KCl, 45; $MgCl_2$, 1; HEPES, 5; EGTA, 10; K-ATP, 3; or alternatively, KCl, 110; KOH, 40; HEPES, 10; EGTA, 10; TEACl, 20; K-ATP, 3; when measuring K^+ or Ca^{2+} currents, respectively (pH = 7.2 in both cases). Membrane currents were recorded with the Axopatch-200B amplifier using the whole-cell configuration of the patch clamp technique. After establishment of a high (1–10 GΩ) resistance seal by gentle suction, the cell membrane beneath the tip of the electrode was disrupted by further suction or by applying 1.5 V electrical pulses for 1 ms. The series resistance was typically 4–8 MΩ before compensation (usually 50–80%). Experiments were discarded when the series resistance was high or substantially increased during the measurement. I_{Kr} was activated by 250 ms depolarizing pulses to +10 mV applied at a rate of 0.05 Hz. The current was characterized as a tail current amplitude determined as the difference between the peak current and the pedestal value observed following repolarization to the holding potential of –40 mV. I_{Ks} was activated by 3 s long depolarizing pulses to +30 mV, delivered at a rate of 0.1 Hz from the holding potential of –40 mV. Tail currents, obtained after repolarization, were used to characterize I_{Ks}. I_{Ca} was activated at +5 mV using 400 ms long depolarizations delivered at a rate of 0.2 Hz from the holding potential of –40 mV. Current amplitudes were determined as differences between peak and pedestal values. Outputs from the clamp amplifier were digitized at 100 kHz under software control (pClamp 6.0, Axon Instruments). Ion currents were normalized to cell capacitance, determined in each cell using short hyperpolarizing pulses from –10 mV to –20 mV.

Action potential voltage clamp

After establishment of whole-cell configuration, action potentials were recorded in current clamp mode from the myocytes superfused with Tyrode solution. The pipette solution was identical to that used for potassium current measurement under conventional voltage clamp conditions. The cells were continuously paced through the recording electrode at a steady stimulation frequency of 1 Hz so as a 1–2 ms gap between the stimulus artefact and the upstroke of the action potential could occur. Ten subsequent action potentials were recorded from each cell, which were analysed online. One of these action potentials, having a duration closest to the average of the 10 recorded action potentials, was delivered to the same cell at an identical frequency as the command voltage after the amplifier had been switched to voltage clamp mode. The current trace obtained under these conditions was a horizontal line positioned at the zero level except for the very short segment corresponding to the action potential upstroke (Fischmeister *et al.*, 1984; Doerr *et al.*, 1990). The effect of ISO was studied in Tyrode solution and in the presence of 10 μM HMR1556 or 1 μM E 4031 in order to prevent activation of the I_{Ks} and I_{Kr}, respectively. The profile of the ISO-activated current was determined by subtracting the pre-drug curve from the post-drug one. This procedure resulted in a downward deflection for an inward (I_{Ca}) and an upward deflection for an outward (I_{Ks} and I_{Kr}) current, corresponding to the known fingerprints of these currents (Varro *et al.*, 2000; Bányász *et al.*, 2003; 2007).

Statistics

Results are expressed as mean ± SEM values. Statistical significance of differences was evaluated using one-way ANOVA followed by Bonferroni's test. Differences were considered significant when P was less than 0.05.

Drugs

ISO was freshly diluted to its final concentration on the day of experiment. Drugs were obtained from Sigma-Aldrich Co. (St. Louis, MO, USA).

Results

Effects of ISO on action potential configuration

ISO induced two characteristic modifications of the canine ventricular action potential: (i) the plateau potential, measured at half time of action potential duration, was shifted significantly towards more positive membrane potential values; and (ii) the duration of action potentials decreased significantly, that is, action potentials shortened. These changes were evident within the concentration range 10–100 nM, and were largely reversible upon washout of ISO (Figure 1). Since 10 nM ISO displayed reproducible and marked effects on action potential characteristics without increasing the incidence of afterdepolarizations, this concentration was used to monitor ISO effects in the presence of various ion channel blockers. As demonstrated in Figure 2, blockade of I_{Kr} by pretreatment with 1 μM E 4031 before application of ISO failed to modify the effect of 10 nM ISO. In contrast, after inhibition of I_{Ks} with 10 μM HMR 1556, the action potential duration induced by 10 nM ISO was increased, while the plateau elevation was preserved. None of these actions were elicited in the absence of functionally active L-type Ca^{2+} channels as indicated by the lack of effect of ISO effect in the presence of 5 μM nisoldipine.

Since the marked interspecies differences in the ISO action may, at least partially, be related to differences in action potential configuration, the possible involvement of action potential morphology in modifying the effects of ISO was further studied by comparing the ISO-induced changes in myocytes of various origins. Although the majority of experiments (if not indicated otherwise) were performed in a mixed myocyte population, containing predominantly midmyocardial cells, the effect of 10 nM ISO was also studied in myocytes digested from either the subepicardial or

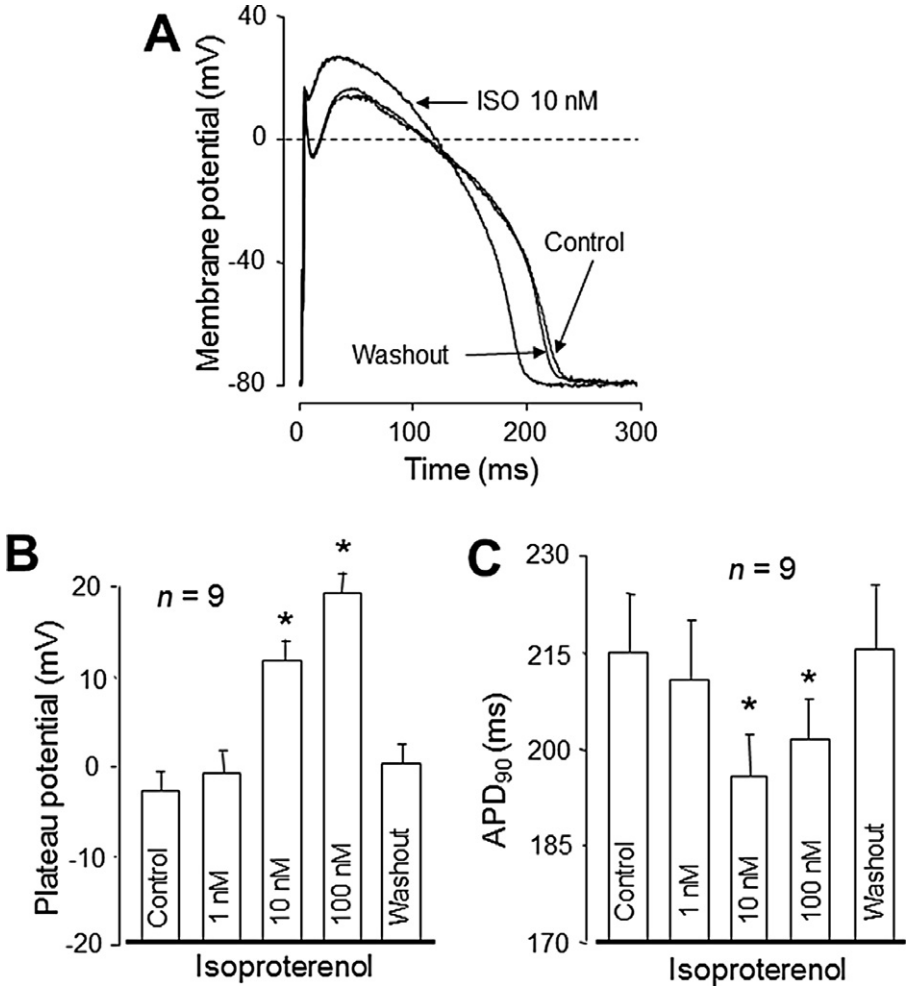

Figure 1

Effect of ISO on action potential configuration. (A) Representative superimposed action potentials recorded in control, in the presence of 10 nM ISO and after washout. Dashed line indicates zero voltage. (B,C) Cumulative concentration-dependent effects of ISO on plateau potential measured at half duration of the action potential, and action potential duration measured at 90% repolarization (APD_{90}). Columns and bars represent mean ± SEM values obtained at 1 Hz, asterisks denote significant changes from control ($P < 0.05$), and n indicates the number of experiments.

subendocardial layers of the middle portion of the left ventricle. As shown in Figure 3A–C, the shortening effect of ISO was totally absent in endocardial cells, while little differences were observed between the epicardial and midmyocardial cells in this regard. Similar results (i.e. the lack of shortening) were obtained when ISO was applied to myocytes that originally had a spike-and-dome action potential morphology, but their transient outward K^+ current (I_{to}) was suppressed by 1 mM 4-aminopyridine (Figure 3D). It is important to note that ISO failed to cause action potential shortening under these conditions at any of the pacing cycle lengths applied (Figure 3C,D). These results clearly demonstrate that the shape of the cardiac action potential has a critical influence on the ISO-induced changes in action potential duration, that is, the shortening can develop only in cells having a spike-and-dome action potential configuration and require both I_{Ca} and I_{Ks} to be functionally active.

Effects of ISO under action potential voltage clamp conditions

Since the profile of an ion current may be quite different when studied under conventional voltage clamp and action potential voltage clamp conditions, the ISO-activated currents were studied using action potential voltage clamp. This technique enables us to record true current profiles flowing during an actual cardiac action potential. Cumulative concentration-dependent effects of ISO on the net membrane current are demonstrated in Figure 4A, where ISO induced a composite current. The initial inward component (downward deflection) is probably mediated by I_{Ca}, while the slow rise of outward current (upward deflection) appears to be associated with I_{Ks} – as suggested by the current–voltage relationship of the ISO-induced composite current depicted in Figure 4B. Enhancement of both currents increased gradually when the

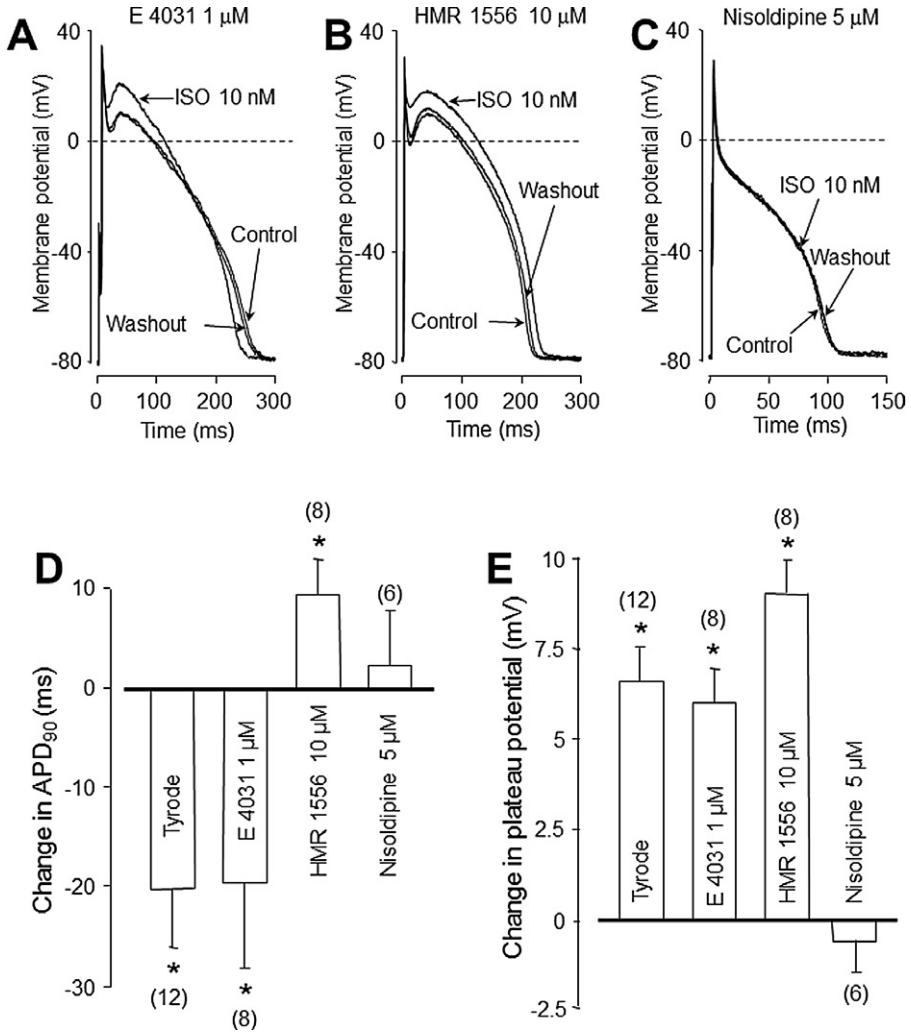

Figure 2

Effect of 10 nM ISO on action potential configuration in the presence of 1 µM E 4031 (A), 10 µM HMR 1556 (B), and 5 µM nisoldipine (C). ISO-induced changes in action potential duration and plateau potential are presented in (D) and (E), respectively. Columns and bars are mean values ± SEM, asterisks indicate significant changes evoked by ISO, and numbers in parentheses denote the number of experiments.

ISO concentration was increased from 1 nM to 1 µM, and – as documented by the lowest current trace in Figure 4A – the effect of ISO was largely reversible.

To develop maximal effects, 100 nM ISO was used in further action potential clamp experiments. Similar to the results obtained with ISO on action potentials, the ISO-induced composite current profiles were largely similar in the absence or presence of 1 µM E 4031 (Figure 5A,B). This indicates that I_{Kr}, although previously shown to be enhanced by ISO (Heath and Terrar, 2000; Harmati *et al.*, 2011), failed to significantly contribute to the ISO-induced current profile. When the ISO was applied after pretreatment with 10 µM HMR 1556, a potent I_{Ks} blocker, the slowly activating outward current component was almost fully abolished, which allowed us to monitor the profile of the ISO-induced inward current (Figure 5C). Since 5 µM nisoldipine failed to block the ISO-induced inward current completely (not shown), 5 mM $NiCl_2$ was combined with 10 µM nisoldipine to suppress inward currents effectively. As indicated in Figure 5D, ISO failed to enhance I_{Ks} under these conditions (i.e. when the plateau of the action potential was depressed due to suppression of inward currents).

Frequency-dependent properties of the ISO-induced current

The effect of ISO on action potential configuration and the underlying ion currents is strongly frequency-dependent in guinea pig (Rocchetti *et al.*, 2006); therefore, we studied the effects of pacing rate on the ISO-induced changes in action potential duration in canine myocytes. Increasing the cycle length of stimulation resulted in an augmentation of the ISO-induced action potential shortening (Figure 6A). When the shortening effect of 100 nM ISO was plotted against the baseline (pre-ISO) value of action potential duration at each pacing cycle length, the shortening effect of ISO appeared to be proportional to the baseline action potential duration. The magnitude of the ISO-induced inward and outward currents was also rate- dependent under action potential voltage

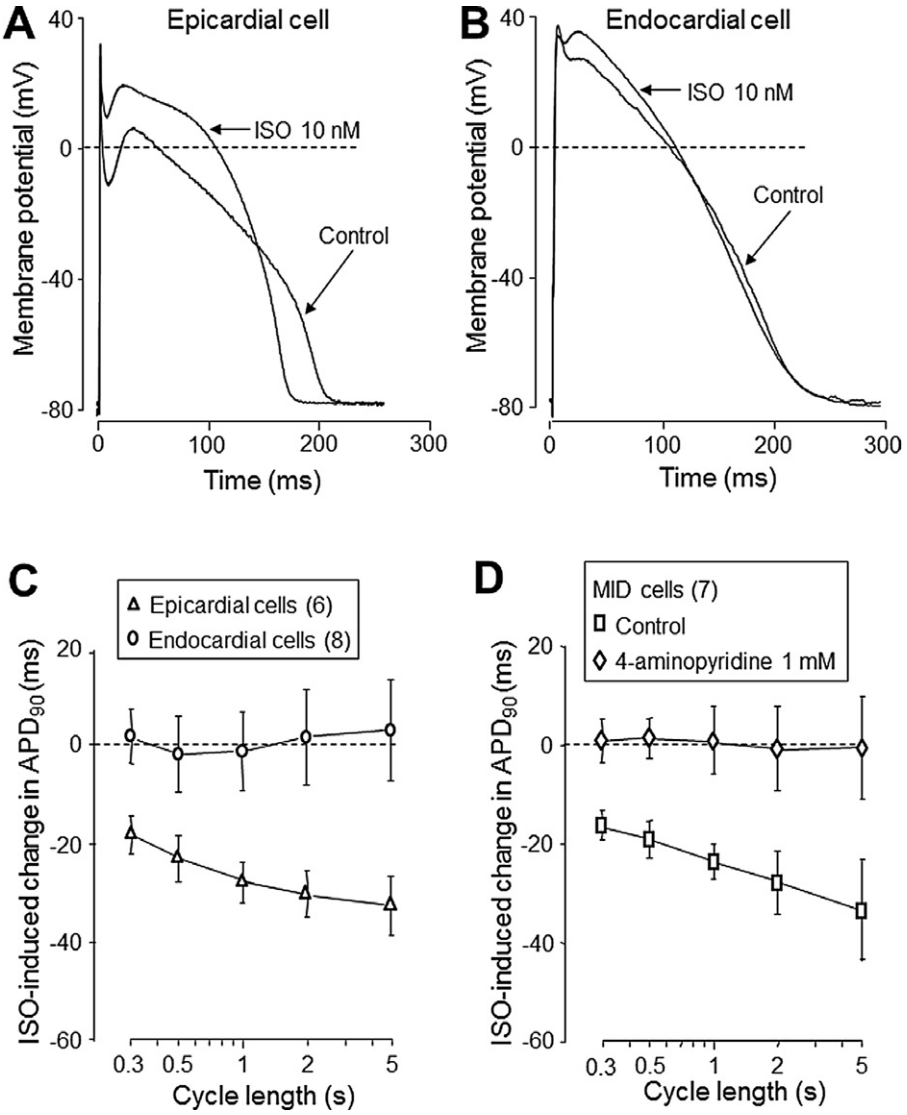

Figure 3

Role of action potential morphology on the ISO-induced changes. (A,B) Superimposed recordings showing the effects of 10 nM ISO in a typical epicardial and endocardial ventricular cell, respectively. (C) Average results of ISO-induced changes in APD obtained from epicardial and endocardial myocytes at various pacing cycle lengths. (D) ISO-induced changes obtained in midmyocardial cells under control conditions and in the presence of 1 mM 4-aminopyridine. Symbols and bars are mean values ± SEM; numbers in parentheses denote the number of experiments.

clamp conditions. Although both components, ie the peak inward as well as peak outward current amplitudes, increased significantly on increasing the pacing cycle length from 0.5 to 1 and 3 s, this increase was more pronounced in the case of inward currents (Figure 6C).

Effects of ISO under conventional voltage clamp conditions

Conventional voltage clamp measurements were designed to determine the magnitude and concentration-dependence of the ISO-induced changes. Effects of cumulative increasing concentrations of ISO on I_{Ks}, I_{Kr} and I_{Ca} were determined, as shown in Figure 7. Superfusion of each ISO concentration lasted for 2–3 min, while washout was for 5–10 min. These incubation and washout periods were sufficient to develop steady-state effects and reversal of effect of each concentration of ISO. The amplitudes of I_{Ks}, I_{Kr} and I_{Ca} increased gradually with increasing ISO concentrations. On fitting these results to the Hill equation, EC_{50} values of 14.5 ± 1.1, 13.7 ± 2.5 and 15.3 ± 3.5 nM were estimated with concomitant Hill coefficients close to unity (0.84 ± 0.05, 1.21 ± 0.28 and 1.32 ± 0.04, respectively). The similarity of the EC_{50} values estimated for I_{Ks}, I_{Kr} and I_{Ca}, indicates the involvement of a common signal transduction mechanism responsible for the ISO-induced activation of all these currents. The Hill plots allowed us to determine maximal ISO effects as well. These were estimated to be 420 ± 4, 133 ± 1 and 340 ± 13% of the respective baseline values obtained for I_{Ks}, I_{Kr} and I_{Ca}, respectively.

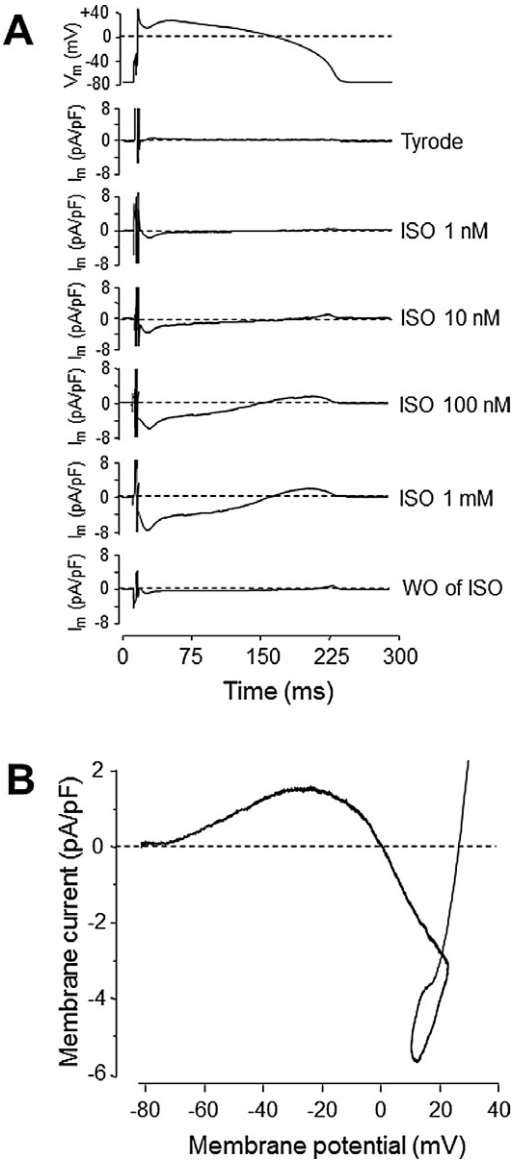

Figure 4

(A) Representative experiment showing cumulative concentration-dependent effects of ISO on membrane currents (I_m) under action potential voltage clamp conditions. The command action potential is displayed in the upper panel, lower the effects of increasing concentrations of ISO are depicted, while the lowest record shows the washout of ISO. Downward and upward deflections indicate inward and outward currents, respectively, activated by ISO. Dashed lines denote zero voltage and zero current as pertinent. (B) Current–voltage relationship (phase-plane trajectory) obtained for the 100 nM ISO-induced current by plotting membrane current against the corresponding membrane potential values throughout the entire action potential.

Finally, the pharmacological suppressibility of the phosphorylated channels was compared to that of the normal, non-phosphorylated channels. In these experiments, 3 μM forskolin was used to mimic sympathetic activation. As demonstrated in Figure 8, the inhibitory effects of HMR 1556, E 4031 and nisoldipine did not differ significantly between normal and phosphorylated channels. The estimated EC_{50} values and Hill coefficients are presented in Figure 8.

Discussion and conclusions

The results of this study indicate that in canine ventricular myocardium, (i) the action potential shortening effect of ISO requires spike-and-dome action potential morphology and an upward shift in the plateau potential, (ii) the shortening is mediated by the ISO-induced activation of I_{Ks}, but is not related to I_{Kr}, (iii) it shows reverse rate-dependent properties, and (iv) ISO activates $I_{Ca,}$ I_{Kr} and I_{Ks} with identical EC_{50} values.

Responses to ISO strongly vary between cardiac preparations and experimental conditions (Munakata *et al.*, 1982; Levesque *et al.*, 1993; Tweedie *et al.*, 1997; Lu *et al.*, 2005). For instance, action potential duration was found to be shortened by ISO in rabbits (Dukes and Vaughan Williams, 1984; Ruiz Petrich *et al.*, 1996), dogs (Volders *et al.*, 2003), cats (Malfatto *et al.*, 1993) and humans (Dorian *et al.*, 2002; Taggart *et al.*, 2003), but prolonged in pigs (Taggart *et al.*, 1990), rats (Ogura *et al.*, 2007) and guinea pigs (Belardinelli and Isenberg, 1983; Rocchetti *et al.*, 2006). This is absolutely in line with the interpretation of our results, that is, that a spike-and-dome action potential configuration, which is a common characteristic of canine, feline and human epicardial and midmyocardial cells, is a prerequisite of the ISO-induced shortening. In addition, an upward shift of the plateau potential has been observed in all mammalian preparations exposed to ISO. The increase in I_{Ca} with the concomitant positive shift in the plateau potential was also evident in the present experiments performed in epicardial or midmyocardial myocytes, while it was less pronounced, although still present, in canine endocardial cells. More importantly, this upward shift of the plateau seems to be a prerequisite of action potential shortening since action potential duration was not modified by ISO in the presence of nisoldipine, when the plateau shift was abolished. In the presence of nisoldipine, one might expect an augmentation of the shortening effect in the absence of an enhanced I_{Ca}. However, as demonstrated in Figure 2, this was not the case but, importantly, the elevation of the plateau was concomitantly abolished. Thus, the ISO-induced shortening of action potential duration required the elevation of plateau, a likely consequence of the simultaneous I_{Ca} enhancement. This positive shift in the plateau potential might stimulate/accelerate the activation of an outward current, which, at least theoretically, could be a mixture of I_{Ks} and I_{Kr} since both currents can be enhanced by ISO (Heath and Terrar, 2000; Volders *et al.*, 2003; Harmati *et al.*, 2011). Since inhibition of I_{Ks} before the application of ISO effectively prevented the shortening, while I_{Kr} blockade failed to do so, it was concluded that activation of I_{Ks} alone was the underlying mechanism for this effect of ISO. This, however, is somewhat surprising because the peak amplitude of I_{Ks} during normal repolarization of canine ventricular myocytes was estimated to be not more than 10 pA, while that of I_{Kr} was mainly 10 times higher, around 80–90 pA (Varro *et al.*, 2000; Hua and Gilmour, 2004; Bányász *et al.*, 2007). Considering that I_{Ks} was augmented by ISO to 420% of its control amplitude, while I_{Kr} was enhanced only to 133% of its baseline value (as demonstrated in Figure 7), the ISO-induced

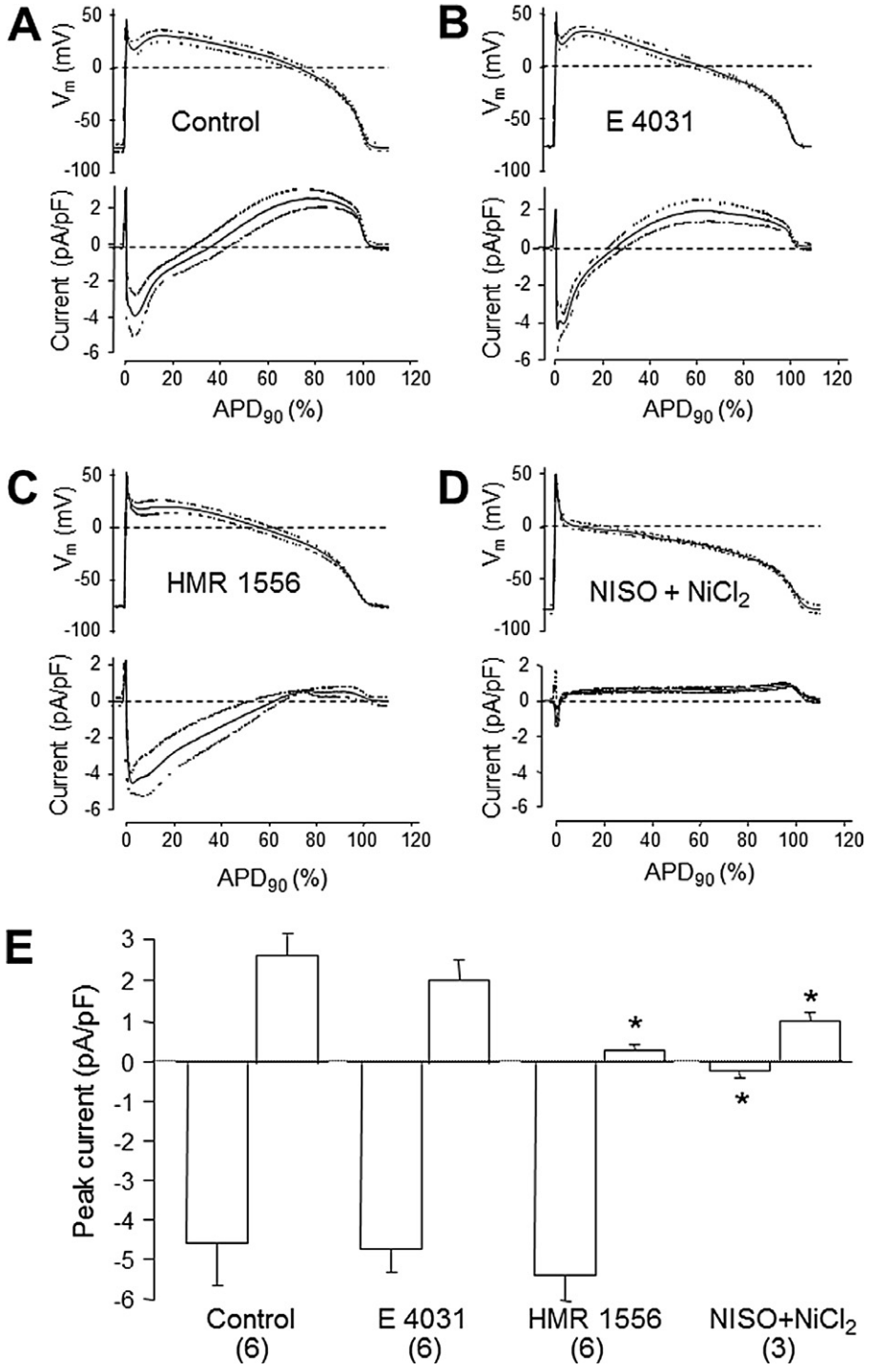

Figure 5

Effects of 100 nM ISO on membrane currents under action potential voltage clamp conditions in Tyrode solution (A), in the presence of 1 μM E 4031 (B), in the presence of 10 μM HMR 1556 (C) and following pretreatment with 10 μM nisoldipine plus 5 mM $NiCl_2$ (D). Action potentials and current records were averaged after normalization to action potential duration (APD_{90} = 100%). Downward and upward deflections indicate inward and outward currents, respectively, activated by ISO. Horizontal dashed lines denote zero voltage and zero current levels, while the dotted lines above and below the voltage and current records indicate 95% confidence limits. (E) Average peak values of the ISO-induced inward and outward currents obtained under various experimental conditions. Columns and bars are mean values ± SEM, asterisks indicate significant changes from control data, and numbers in parentheses denote the number of experiments.

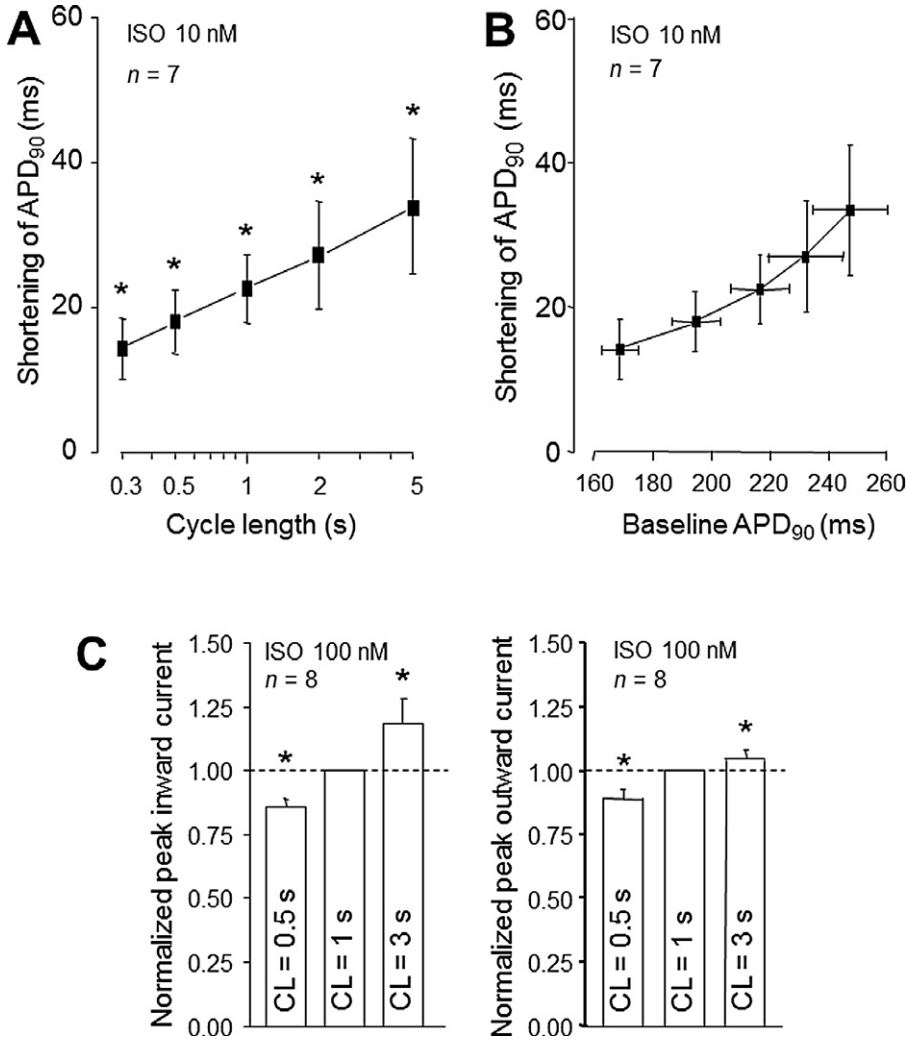

Figure 6

Rate-dependent properties of the ISO effect. (A) ISO-induced shortening of action potential duration (APD_{90}) as a function of the pacing cycle length. (B) Results from the same experiments: here, the shortening effect of 10 nM ISO was plotted against the respective baseline (pre-ISO) value of APD_{90} measured at each cycle length. (C) Results of action potential voltage clamp experiments performed with 100 nM ISO at three pacing cycle lengths (0.5, 1 and 3 s). Peak values of inward and outward currents obtained at cycle lengths of 0.5 s and 3 s were normalized to those measured at a cycle length of 1 s. Columns and bars denote mean values ± SEM; asterisks indicate significant changes from the 1 Hz data.

components of the two currents should be comparable in size. If we take into account the finding that ISO failed to shorten action potentials in the presence of nisoldipine, when both I_{Ks} and I_{Kr} could be freely stimulated by ISO, it is clear that some additional alteration beyond the direct effect of ISO on I_{Ks} and I_{Kr} is also needed to induce shortening. This crucial change is likely to be the elevation of plateau potential due to enhancement of I_{Ca}. I_{Kr} is almost fully activated at normal plateau potential; therefore, its contribution to terminal repolarization is less influenced by the plateau voltage compared to I_{Ks}, the activation of which is sharply increased by positive voltage shifts beyond this level (Horváth *et al.*, 2006; Jost *et al.*, 2009; Severi *et al.*, 2009). As a consequence, the relative contribution of I_{Ks} will be dominant under conditions where the plateau is markedly elevated. This conclusion accords with those of Varro *et al.* (2000) and Volders *et al.* (2003), who suggested that the contribution of I_{Ks} to canine ventricular repolarization is almost negligible at rest but is an important factor following sympathetic stimulation.

Our most important result was to show that ISO shortens action potentials only in myocytes displaying a spike-and-dome action potential configuration. Thus, no shortening was observed in endocardial cells or in myocytes pretreated with 1 mM 4-aminopyridine. This phenomenon can be attributed to ISO-induced indirect changes in I_{Ks} kinetics. In epicardial cells, the strongly positive voltage of the late dome probably results in a larger I_{Ks} amplitude than in the case of an endocardial cell, which shows less positive membrane potential values at this time (Rudy and Silva, 2006). This might explain why cardiac action potentials can be lengthened by ISO in guinea pigs, but not in canine, feline, or human epicardial tissues, as predicted by Malfatto *et al.* (2010). The asymmetrical ISO effect (shortening of epicardial but not endocardial action potential duration) may increase

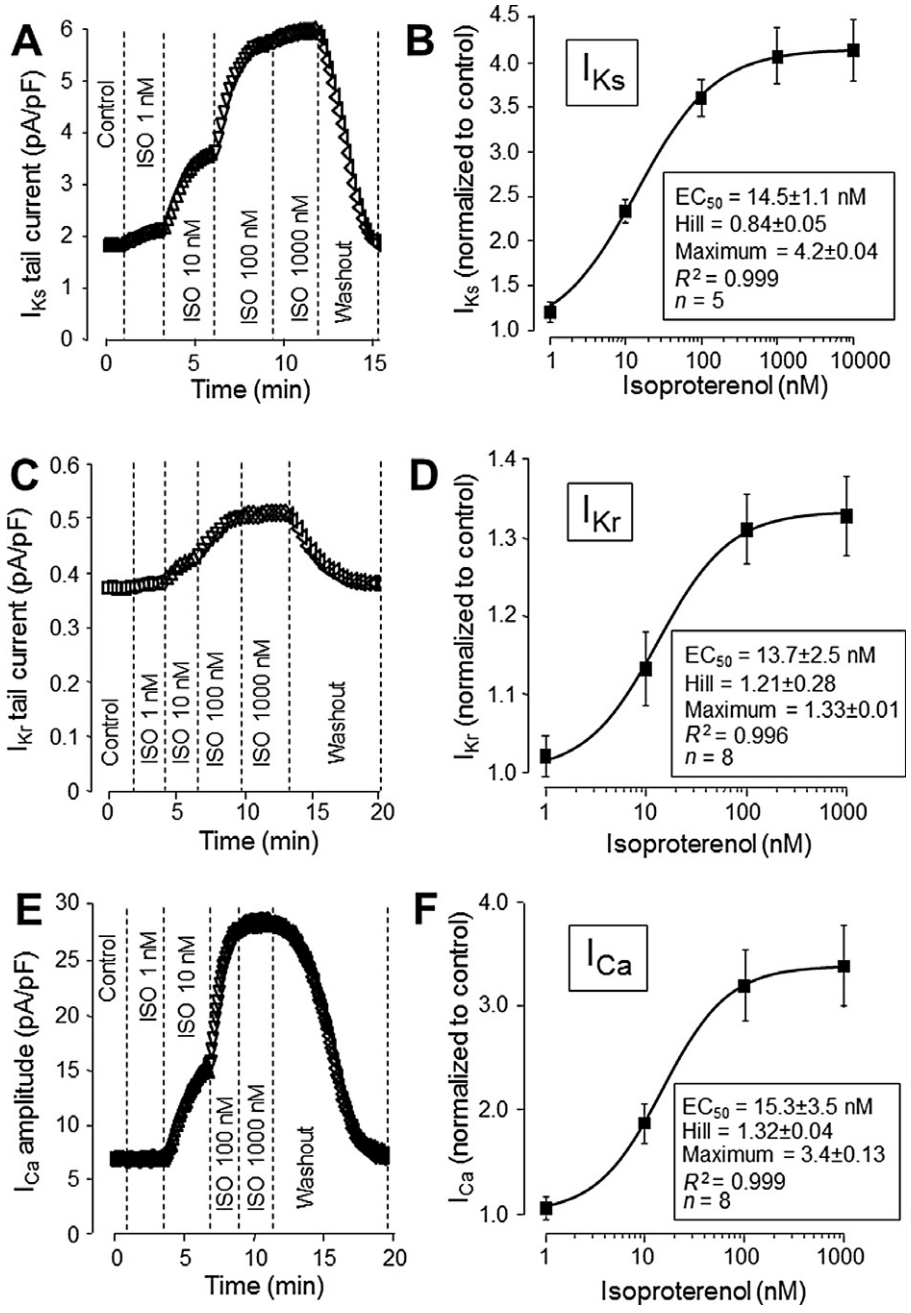

Figure 7

Cumulative concentration-dependent effects of ISO on I_{Ks} (A, B), I_{Kr} (C,D) and I_{Ca} (E,F) under conventional voltage clamp conditions. Each left panel depicts a representative experiment, while average results are summarized in the right panels. Results of Hill plots are presented in the insets showing EC_{50} values, Hill coefficients, maximal current levels normalized to baseline values, regression coefficient and number of measurements. Symbols and bars denote mean ± SEM.

the transmural dispersion through the ventricular wall during sympathetic stimulation, which may contribute to increased arrhythmia propensity under these conditions. Furthermore, since the ISO-induced shortening was increased with lengthening of the pacing cycle length, the increased dispersion will be further aggravated when the ISO challenge occurs during bradycardia, thus increasing the risk of the 'alarm-induced' sudden cardiac death. It must be mentioned, however, that the reverse rate-dependent nature of the ISO effect is probably not related to the known rate-dependent properties of the underlying ion currents, since in our experiments, the augmentation of I_{Ca} evoked by increasing the cycle lengths from 0.5 to 2 s was much greater than that of I_{Ks} (Figure 6C). The explanation for this is based on the general behaviour of cardiac tissues, which produce reverse rate-dependent alterations in action potential duration (either lengthening or shortening) in response to prolongation of baseline action potential duration (Bányász

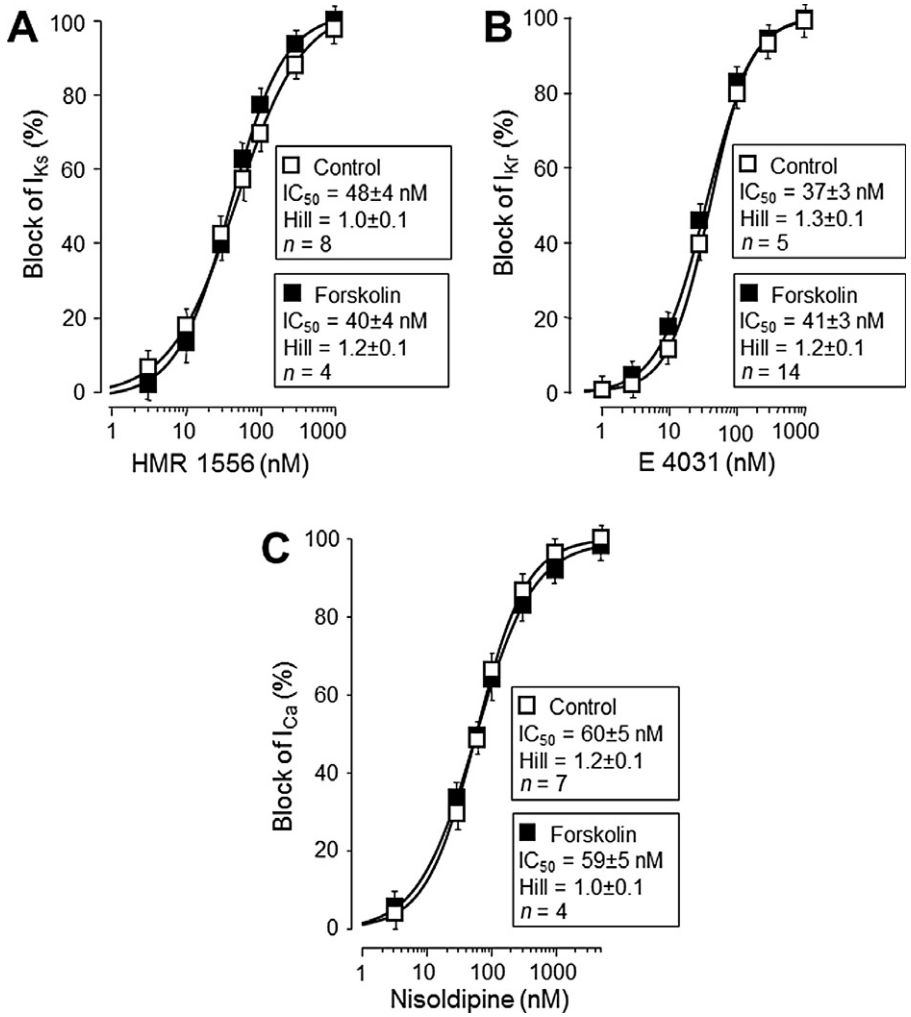

Figure 8

Pharmacological suppressibility of phosphorylated (by 3 μM forskolin) and unphosphorylated (control) channels. Dose-response curves obtained under conventional voltage clamp conditions with HMR 1556 for I_{Ks} (A), with E 4031 for I_{Kr} (B) and with nisoldipine for I_{Ca} (C) were determined in a cumulative manner. Results of Hill plots are in the insets. Results of Hill plots are presented in the insets showing EC_{50} values, Hill coefficients, and number of measurements.

et al., 2009; 2011; Bárándi *et al.*, 2010) and is in line with the results of Figure 6B.

It is worthy of note that the profile of I_{Ca} observed in the presence of ISO under action potential voltage clamp conditions (see Figures 4A and 5A) was basically different from that previously recorded from untreated canine myocytes (Bányász *et al.*, 2003). The current was permanently active throughout the early plateau phase in our ISO-treated myocytes, resembling the baseline I_{Ca} profiles recorded from guinea pig ventricular cells using action potential voltage clamp (Arreola *et al.*, 1991; Linz and Meyer, 1998; 2000). ISO-induced phosphorylation of L-type Ca^{2+} channels was reported to follow markedly altered gating kinetics with decreased probability of mode 0, but higher probability of mode 2 gating, resulting in a decreased peak amplitude combined with an increased window component active at the plateau level (Striessnig, 1999; Catterall, 2000; Kamp and Hell, 2000). This is exactly what we observed in our action potential clamp experiments performed in canine ventricular cells. However, there is a prominent difference between the ISO-activated I_{Ca} in dogs and guinea pigs; namely, that I_{Ca} persists throughout the entire action potential in ISO-treated guinea pig myocytes (Rocchetti *et al.*, 2006), while it showed a clear-cut decaying tendency during the plateau in dogs (see Figure 5C). This difference may probably contribute to the interspecies differences observed with ISO between canine and guinea pig cardiac cells.

To explain the marked variability of the ISO-induced changes in various mammalian species, it was previously claimed that sympathetic stimulation modulates cardiac ion currents using different (i.e. involving more than one) signal transduction pathways. In this is true, however, the EC_{50} values of ISO obtained for I_{Ca}, I_{Ks} and I_{Kr} should be different, whereas we observe that ISO activated $I_{Ca,}$ I_{Kr} and I_{Ks} with practically identical EC_{50} values and Hill coefficients; only differences in the magnitude of activation were found. This suggests that one single mechanism (probably the cAMP/PKA pathway) mediates the effects of sympathetic

stimulation on $I_{Ca,}$ I_{Kr} and I_{Ks} uniformly in canine ventricular cardiomyocytes.

The involvement of stimulation of I_{Ks}, but not I_{Kr}, in the ISO-induced shortening of the canine, and probably human, ventricular action potentials has important clinical implications. Class 3 anti-arrhythmics, drugs known to block typically I_{Kr}, may carry the risk of enhanced incidence of early afterdepolarizations resulting often in torsade de pointes type arrhythmias (Roden, 2001), clearly as a consequence of the compromised repolarization reserve (Biliczki *et al.*, 2002; Jost *et al.*, 2005). Sympathetic activity is also known to increase the incidence of early afterdepolarizations, thus a combination of K^+ channel blockade with sympathetic stimulation was shown to be extremely dangerous (Nalivaiko *et al.*, 2004). Application of I_{Ks} blockers as a new generation of class 3 anti-arrhythmics has been proposed due to their favourable rate-dependent properties (Bauer *et al.*, 2000; Salata *et al.*, 2004). Extrapolation of our canine results to humans supports the conclusion that these agents may be even more dangerous in cases of an inherited or acquired form of long QT syndrome than the 'classic' class 3 drugs, since these patients treated with an I_{Ks} blocker will lack the ultimate mechanism of repolarization following a strong sympathetic activation. This is true in spite of the fact that I_{Ks} is thought to be an insignificant repolarizing current under baseline conditions. These considerations must be kept in mind when developing new anti-arrhythmic agents or strategies.

Acknowledgements

Financial support for the studies was provided by grants from the Hungarian Research Fund (OTKA-K100151, OTKA-PD101171, OTKA-K73160, CNK-77855), and the Hungarian Government (TÁMOP-4.2.1/B-09/1/KONV-2010-007). The authors thank Mrs Vighné Katalin Horváth for excellent technical assistance.

Conflict of interest

None.

References

Arreola J, Dirksen RT, Shieh RC, Williford DJ, Sheu SS (1991). Ca^{2+} current and Ca^{2+} transients under action potential clamp in guinea pig ventricular myocytes. Am J Physiol 261: C393–C397.

Bányász T, Fülöp L, Magyar J, Szentandrássy N, Varró A, Nánási PP (2003). Endocardial versus epicardial differences in L-type calcium current in canine ventricular myocytes studied by action potential voltage clamp. Cardiovasc Res 58: 66–75.

Bányász T, Magyar J, Szentandrássy N, Horváth B, Birinyi P, Szentmiklósi J *et al.* (2007). Action potential clamp fingerprints of K^+ currents in canine cardiomyocytes: their role in ventricular repolarization. Acta Physiol Scand 190: 189–198.

Bányász T, Horváth B, Virág L, Bárándi L, Szentandrássy N, Harmati G *et al.* (2009). Reverse rate dependency is an intrinsic property of canine cardiac preparations. Cardiovasc Res 84: 237–244.

Bányász T, Bárándi L, Virág L, Szentandrássy N, Márton I, Zaza A *et al.* (2011). Mechanism of reverse rate-dependent action of cardioactive agents. Curr Med Chem 18: 3597–3606.

Bárándi L, Virág L, Jost N, Horváth Z, Koncz I, Papp R *et al.* (2010). Reverse rate-dependent changes are determined by baseline action potential duration in mammalian and human ventricular preparations. Basic Res Cardiol 105: 315–323.

Bauer A, Becker R, Freigang KD, Senges JC, Voss F, Kraft P *et al.* (2000). Electrophysiologic effects of the new I_{Ks}-blocking agent chromanol 293b in the postinfarction canine heart. Preserved positive use-dependence and preferential prolongation of refractoriness in the infarct zone. Basic Res Cardiol 95: 324–332.

Belardinelli L, Isenberg G (1983). Actions of adenosine and isoproterenol on isolated mammalian ventricular myocytes. Circ Res 53: 287–297.

Biliczki P, Virág L, Iost N, Papp JG, Varró A (2002). Interaction of different potassium channels in cardiac repolarization in dog ventricular preparations: role of repolarization reserve. Br J Pharmacol 137: 361–368.

Catterall WA (2000). Structure and regulation of voltage-gated Ca^{2+} channels. Annu Rev Dev Biol 16: 521–555.

Doerr T, Denger R, Doerr A, Trautwein W (1990). Ionic currents contributing to the action potential in single ventricular myocytes of the guinea pig studied with action potential clamp. Pflugers Arch 416: 230–237.

Dorian P, Dunnmon P, Elstun L, Newman D (2002). The effect of isoproterenol on the class III effect of azimilide in humans. J Cardiovasc Pharmacol Ther 7: 211–217.

Dukes ID, Vaughan Williams EM (1984). Effects of selective α_1, α_2, β_1 and β_2 adrenoceptor stimulation on potentials and contractions in the rabbit heart. J Physiol 355: 523–546.

Fischmeister R, DeFelice LJ, Ayer RK, Levi R, DeHaan RL (1984). Channel currents during spontaneous action potentials in embryonic chick heart sells. The action potential patch clamp. Biophys J 46: 267–271.

Harmati G, Bányász T, Bárándi L, Szentandrássy N, Horváth B, Szabó G *et al.* (2011). Effects of β-adrenergic stimulation on delayed rectifier K^+ currents in canine ventricular cardiomyocytes. Br J Pharmacol 162: 890–896.

Harvey RD, Clark CD, Hume JR (1990). Cl^- current in mammalian cardiac myocytes: novel mechanism for autonomic regulation of action potential duration and resting membrane potential. J Gen Physiol 95: 1077–1102.

Heath BM, Terrar DA (2000). Protein kinase C enhances the rapidly activating delayed rectifier potassium current, I_{Kr}, through a reduction in C-type inactivation in guinea-pig ventricular myocytes. J Physiol 522: 391–402.

Horváth B, Magyar J, Szentandrássy N, Birinyi P, Nánási PP, Bányász T (2006). Contribution of I_{Ks} to ventricular repolarization in canine myocytes. Pflugers Arch 452: 698–706.

Hua F, Gilmour RF (2004). Contribution of I_{Kr} to rate-dependent action potential dynamics in canine endocardium. Circ Res 94: 810–819.

January CT, Riddle MJ (1990). Early afterdepolarizations: mechanism of induction and block, a role for L-type Ca^{2+} current. Circ Res 64: 977–990.

Jost N, Virag L, Bitay M, Takacs J, Lengyel C, Biliczki P *et al.* (2005). Restricting excessive cardiac action potential and QT prolongation: a vital role for I_{Ks} in human ventricular muscle. Circulation 112: 1392–1399.

Jost N, Acsai K, Horváth B, Bányász T, Bitay M, Bogáts G *et al.* (2009). Contribution of I_{Kr} and I_{K1} to ventricular repolarization in canine and human myocytes. Is there any influence of action potential duration? Basic Res Cardiol 104: 33–41.

Kamp TJ, Hell JW (2000). Regulation of cardiac L-type calcium channels by protein kinase A and protein kinase C. Circ Res 87: 1095–1102.

Katsube Y, Yokoshiki H, Nguyen L, Sperelakis N (1996). Differences in isoproterenol stimulation of Ca^{2+} current of rat ventricular myocytes in neonatal compared to adult. Eur J Pharmacol 317: 391–400.

Kilkenny C, Browne W, Cuthill IC, Emerson M, Altman DG (2010) NC3Rs Reporting Guidelines Working Group. Br J Pharmacol 160:1577–1579.

Levesque PC, Clark CD, Zakarov SI, Rosenshtraukh LV, Hume JR (1993). Anion and cation modulation of the guinea-pig ventricular action potential during beta-adrenoceptor stimulation. Pflugers Arch 424: 54–62.

Linz KW, Meyer R (1998). Control of L-type calcium current during the action potential of guinea-pig ventricular myocytes. J Physiol 513: 425–442.

Linz KW, Meyer R (2000). Profile and kinetics of the L-type calcium current during the cardiac ventricular action potential compared in guinea-pigs, rats and rabbits. Pflugers Arch 439: 588–599.

Lu HR, Vlaminckx E, Van De Water A, Gallacher DJ (2005). Both beta-adrenergic receptor stimulation and cardiac tissue type have important roles in elucidating the functional effects of I_{Ks} channel blockers *in vitro*. J Pharmacol Toxicol Methods 51: 81–90.

McDonald TF, Pelzer S, Trautwein W, Pelzer DJ (1994). Regulation and modulation of calcium channels in cardiac, skeletal, and smooth muscle cells. Physiol Rev 74: 365–507.

McGrath J, Drummond G, Kilkenny C, Wainwright C (2010). Guidelines for reporting experiments involving animals: the ARRIVE guidelines. Br J Pharmacol 160: 1573–1576.

Magyar J, Szentandrássy N, Bányász T, Fülöp L, Varró A, Nánási PP (2002). Effects of thymol on calcium and potassium currents in canine and human ventricular cardiomyocytes. Br J Pharmacol 136: 330–338.

Malfatto G, Zaza A, Schwartz PJ (1993). Parasympathetic control of cycle length dependence of endocardial ventricular repolarisation in the intact feline heart during steady state conditions. Cardiovasc Res 27: 823–827.

Malfatto G, Rocchetti M, Zaza A (2010). The role of the autonomic system in rate-dependent repolarization changes. Heart Rhythm 7: 1700–1703.

Munakata K, Dominic JA, Surawicz B (1982). Variable effects of isoproterenol on action potential duration in guinea-pig papillary muscle: differences between nonsteady and steady state; role of extracellular calcium concentration. J Pharmacol Exp Ther 221: 806–814.

Nalivaiko E, De Pasquale CG, Blessing WW (2004). Ventricular arrhythmias triggered by alerting stimuli in conscious rabbits pre-treated with dofetilide. Basic Res Cardiol 99: 142–151.

Ogura K, Miake J, Sasaki N, Iwai C, Bahrudin U, Li P *et al.* (2007). Inhibition of beta-adrenergic signaling by intracellular AMP is independent of cell-surface adenosine receptors in rat cardiac cells. J Mol Cell Cardiol 43: 648–652.

Rocchetti M, Freli V, Perego V, Altomare C, Mostacciuolo G, Zaza A (2006). Rate dependency of beta-adrenergic modulation of repolarizing currents in the guinea-pig ventricle. J Physiol 574: 183–193.

Roden DM (2001). Pharmacogenetics and drug-induced arrhythmias. Cardiovasc Res 50: 224–231.

Rudy Y, Silva JR (2006). Computational biology in the study of cardiac ion channels and cell electrophysiology. Q Rev Biophys 39: 57–116.

Ruiz Petrich E, Ponce Zumino A, Schanne OF (1996). Early action potential shortening in hypoxic hearts: role of chloride current(s) mediated by catecholamine release. J Mol Cell Cardiol 28: 279–290.

Salata JJ, Selnick HG, Lynch JJ (2004). Pharmacological modulation of I_{Ks}: potential for antiarrhythmic therapy. Curr Med Chem 11: 29–44.

Severi S, Corsi C, Rocchetti M, Zaza A (2009). Mechanisms of beta-adrenergic modulation of I_{Ks} in the guinea-pig ventricle: insights from experimental and model-based analysis. Biophys J 96: 3862–3872.

Stengl M, Volders PGA, Thomsen MB, Spatjens RLHMG, Sipido KR, Vos M (2003). Accumulation of slowly activating delayed rectifier potassium current (I_{Ks}) in canine ventricular myocytes. J Physiol 551: 777–786.

Striessnig J (1999). Pharmacology, structure and function of cardiac L-type Ca^{2+} channels. Cell Physiol Biochem 9: 242–269.

Szabó G, Szentandrássy N, Bíró T, Tóth IB, Czifra G, Magyar J *et al.* (2005). Asymmetrical distribution of ion channels in canine and human left ventricular wall: epicardium versus midmyocardium. Pflugers Arch 450: 307–316.

Szentadrássy N, Bányász T, Bíró T, Szabó G, Tóth B, Magyar J *et al.* (2005). Apico-basal inhomogeneity in distribution of ion channels in canine and human ventricular myocardium. Cardiovasc Res 65: 851–860.

Szentandrássy N, Harmati G, Bárándi L, Simkó J, Horváth B, Magyar J *et al.* (2011). Effects of rosiglitazone on action potential configuration and ion currents in canine ventricular cells. Br J Pharmacol 163: 499–509.

Taggart P, Sutton P, Lab M, Dean J, Harrison F (1990). Interplay between adrenaline and interbeat interval on ventricular repolarization in intact heart *in vivo*. Cardiovasc Res 24: 884–895.

Taggart P, Sutton P, Chalabi Z, Boyett MR, Simon R, Elliott D *et al.* (2003). Effect of adrenergic stimulation on action potential duration restitution in humans. Circulation 107: 285–289.

Tweedie D, O'Gara P, Harding SE, MacLeod KT (1997). The effect of alterations to action potential duration on beta-adrenoceptor-mediated aftercontractions in human and guinea-pig ventricular myocytes. J Mol Cell Cardiol 29: 1457–1467.

Van der Heyden MA, Wijnhoven TJ, Opthof T (2005). Molecular aspects of adrenergic modulation of cardiac L-type Ca^{2+} channels. Cardiovasc Res 65: 28–39.

Varro A, Balati B, Iost N, Takacs J, Virag L, Lathrop DA *et al.* (2000). The role of the delayed rectifier component I_{Ks} in dog ventricular muscle and Purkinje fibre repolarization. J Physiol 523: 67–81.

Volders PGA, Stengl M, van Opstal JM, Gerlach U, Spatjens RLHMG, Beekman JDM *et al.* (2003). Probing the contribution of I_{Ks} to canine ventricular repolarization: key role for β-adrenergic receptor stimulation. Circulation 107: 2753–2760.